CHARACTERISATION OF CONSTRAINT EFFECTS BASED ON MICROMECHANICAL MODELING

Huang Yuan & Dietmar Kalkhof*

It is known that material failure depends on specimen geometry and loading configuration. The two-parameter characterizations can quantify variations of the crack tip fields without relating material failure process. In the present paper we use the Gurson-Tvergaard-Needleman damage model to check the correlation between the damage evolution around the crack tip and the known constraint parameters. It is shown that a crack does not grow along the symmetric plane even under the mode I loading conditions. The crack growth angle at initiation increases with the applied T stresses if $0.5<|T/\sigma_o|\leq 1$. For $|T/\sigma_o|\leq 0.5$, however, the crack angle hardly changes. After small amount of crack growth the damage zone develops toward the symmetrical plane. For the same J value the material damage is increasing with the applied T-stresses. Under plane strain conditions the evolution process of the damage zone can be described by both J and T.

INTRODUCTION

Extensive computational and experimental efforts have shown that the material failure depends on specimen geometry and loading configuration, which was termed as constraint effects in the fracture mechanics community. The known crack assessment methodologies, e.g. J - T [1] and J - Q [2], have been confirmed under nearly plane strain loading conditions, that is, so-called in-plane constraint effects can be accurately quantified by an additional parameter, e.g. T or Q. Effects from the out-of-plane, however, can only partially or even not be caught by using these methods. Detailed three-dimensional computations [3, 4] reveal that the crack front is effected by the nearly plane stress state increasingly with loading and the nearly plane strain crack field around a three-dimensional crack front shrinks. These effects cannot be described by the known second parameters. To understand the limitations of the two-parameter characterizations and to generate a more general description for the material failure process, we need more detailed theoretical and computational knowledge about crack tip fields. It becomes important to find out the relationships between the global fracture parameters and the local material failure process [5].

*Laboratory for Safety and Accident Research, Paul Scherrer Institute, CH-5232 Villigen PSI, Switzerland

In the present paper we use the Gurson-Tvergaard-Needleman (GTN) damage model [8, 9] to check the correlation between the damage evolution around the crack tip and the known fracture parameters. Upon detailed finite element computations we are studying interdependence of material failure and the constraint effects.

MODELING

In this work the ductile materials behavior is modeled by porous metal plasticity first introduced by Gurson [8] and modified by Tvergaard and Needleman [9, 10]. The plastic potential is written as

$$\Phi(\sigma_e, \sigma_m, \sigma_M, f^*) = \left(\frac{\sigma_e}{\sigma_M}\right)^2 + 2q_1 f^* \cosh\left(\frac{3q_2\sigma_m}{2\sigma_M}\right) - [1 + (q_1 f^*)^2] = 0, \quad (1)$$

with

$$\dot{f} = \dot{f}_{Nucl} + \dot{f}_{Growth}, \quad (2)$$

$$\dot{f}_{Nucl} = \frac{f_N}{\sqrt{2\pi}s_N} \exp\frac{1}{2}\left(\frac{\bar{\varepsilon}^{pl}_M - \varepsilon_N}{s_N}\right)^2 \dot{\bar{\varepsilon}}^{pl}_M, \quad (3)$$

$$\dot{f}_{Growth} = (1 - f)\dot{\varepsilon}^{pl}_{ij}\delta_{ij} \quad (4)$$

where σ_e is the macroscopic effective von Mises stress and σ_m is the macroscopic mean stress; q_1, q_2 are the fitting parameters introduced by Tvergaard to improve numerical accuracy of the model. σ_M is microscopic yield stress of the matrix material. In this study the matrix material has a initial yield stress σ_0 and a true stress-logarithmic strain relation as

$$E\varepsilon = \begin{cases} \sigma & \text{for } \sigma < 1, \\ \sigma + \alpha(\sigma^n - 1) & \text{for } \sigma \geq 1. \end{cases} \quad (5)$$

Here the stress, σ, and Young's modulus, E, are non-dimensionalized by σ_0. $n = 10$ describes the plastic strain hardening exponent. The matrix material is assuming isotropic and may be described by the J_2 flow theory of plasticity. The void volume fraction

$$f^* = \begin{cases} f & \text{for } f \leq f_c \\ f_c + \dfrac{f_U - f_c}{f_f - f_c}(f - f_c) & \text{for } f > f_c \end{cases} \quad (6)$$

is defined as the ratio of all cavity volume over body volume and is an internal variable to describe material damage. More detailed explanation of material parameters in (1) - (6) about the micromechanical damage model are referred to the works of Tvergaard and Needleman [9, 10]. This material model is implemented into the general FE code ABAQUS using the UMAT interface.

For our computations the initial void volume fraction, $f_0 = 0$, will not change our final results. Further material parameters of GTN model are $f_c = 0.15$, $f_f = 0.3$, $f_N = 0.04$, $f_U = 0.667$, $\varepsilon_N = 0.3$, $s_N = 0.1$, $q_1 = 1.5$, $q_2 = 1$, $E/\sigma_0 = 300$ and $\alpha = 1$, respectively.

To study effects of applied load biaxiality on material failure, we consider a mode I crack tip field modeled by the modified boundary layer (BLF) under plane strain conditions. The remote loads are given by the first two terms of the elastic asymptotic solution in the form

$$\sigma_{ij}(r,\vartheta) = \frac{K}{\sqrt{2\pi r}} f_{ij}(\vartheta) + T\delta_{1i}\delta_{1j}, \tag{7}$$

where r denotes the radial distance to the crack tip. The significance of this T-term for the size and shape of the plastic zone size under small scale yielding (SSY) conditions have been studied extensively in [1, 6, 7]. The T-stress is supposed to characterize effects of the in-plane constraint in elastic-plastic fracture mechanics.

It is known that the local assumption in continuum mechanics makes stress and strain distributions scalable by some geometrical dimension. It follows that the prediction of material failure based on a local mechanics model is mesh-dependent, especially for crack analyses [11, 12]. Actually, all stress/strain fields in a elastic-plastic solids and so the predictions of the crack initiation based on the continuum mechanics can be linearly scaled by a characteristic dimension of the FE model [13]. One may not hope to give an accurate prediction of material failure without introducing a microstructural characteristic length scale. This problem can be overcome only by using non-local formulation in continuum mechanics which beyond our scope of this paper. In crack damage modeling the blunting radius of the crack tip plays a key-role. To study the crack tip fields we use a very fine FE mesh as shown in Fig. 1. Our numerical experiments using mesh with 12 to 36 element sectors around the tip from 0 to 180° confirm that the crack initiates at numerically similar J values if the length of the smallest elements ahead of the crack tip is set uniformly. The element number around the crack tip does not substantially affect the final prediction.

To diminish the model effects, the cracked geometry is discretized using a similar mesh structure for all computations. The radius of the blunted crack tip, δ_0, is 10^{-7} times the remote radius of BLF, R_0. The radial length of the elements directly near to the crack tip is equal to $\delta_0/2$. The mesh in $r > 10\delta_0$ is scaled exponentially in the radial direction. There are 12 to 36 sectors of elements within the angular region from 0 to 180° in the crack-tip region. Both 4-node B-bar elements as well as 8-nodal isoparametric elements are used in different computations. Because of symmetry we only have to model the upper plane. A typical mesh with 24 elements around the tip is plotted in Fig. 1. The ABAQUS general-purpose finite element program has been used for the computations.

RESULTS

From fracture mechanics we know that the J-integral in the modified boundary layer formulation does not depend on the transverse stress T. It implies that the crack tip fields are characterized by both J and T. In our computations the transverse stresses τ $(= T/\sigma_0)$ are given and the applied stress intensity factor J or K of Eq. (7) increases from $J/(\delta_0\sigma_0) = 3.33$ to 20. We have computed with $\tau = -1, -0.75, -0.5, -0.25, 0, 0.25, 0.5, 0.75, 1$ and different meshes under small scale

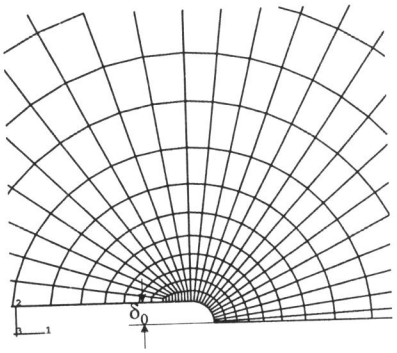

Figure 1: Details of the finite element mesh around the blunted crack tip. The mesh shown in the figure consists of 24 elements around the tip.

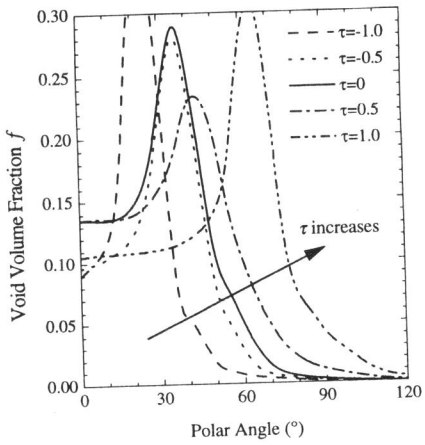

Figure 2: Angular distributions of the void volume fraction under different applied transverse T-stresses at $J/(\sigma_0\delta_0) = 9.63$ and $r = 2\delta_0$. The mesh contains 24 quadratic element sectors around the tip.

yielding condition ($r_{plastic} < 0.05R_0$). It is observed that the crack initiates at $J/(\delta_0\sigma_0) \geq 5.0$ and the exact values essentially vary with T.

The T-stress changes crack initiation since the developments of the damage zone around the crack tip are sensitive to the biaxial loading. Fig. 2 shows angular distributions of the void volume fraction f at $r = 2\delta_0$ and $J/(\delta_0\sigma_0) = 9.6$. The applied transverse stresses are $\tau = -1, -0.5, 0, 0.5$ and 1.0, respectively. The curves are smoothend using spline functions. From the figure we learn that the crack does not initiates along the symmetrical plane ($\vartheta = 0$). The crack growth angle at initiation, ϑ_{crack}, depends continuously on the loading biaxialities, τ.

More detailed FE-computations using different meshes and element types in Fig. 3 show that ϑ_{crack} is only slightly affected by FE models. In the figure the solid symbols and open symbols denote the quadratic and linear isoparametric element meshes, respectively. With increasing the transverse stresses ϑ_{crack} moves towards to $\vartheta = 60°$. For $|\tau| \leq 0.5$ ϑ_{crack} hardly changes. The crack growth angle can be approximated by a third-order polynomial as

$$\vartheta_{crack} = 34 + 8\tau + 6\tau^2 + 13\tau^3. \tag{8}$$

The coefficients of the polynomial are determined using the least square fitting and seem only effected by the parameters of the GTN-model. Numerical scattering of the prediction above is smaller than the element sector angles of FE-mesh around the crack tip.

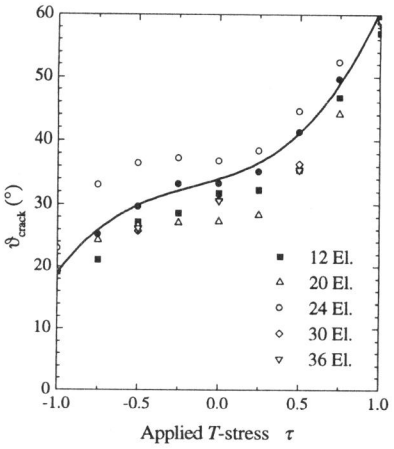

Figure 3: Crack growth angles, ϑ_{crack}, as a function of the applied transverse T-stresses using different FE-meshes. The curve legends denote the numbers of element sectors around the tip. The solid and open symbols stand for the quadratic isoparametric and linear B-bar element meshes, respectively.

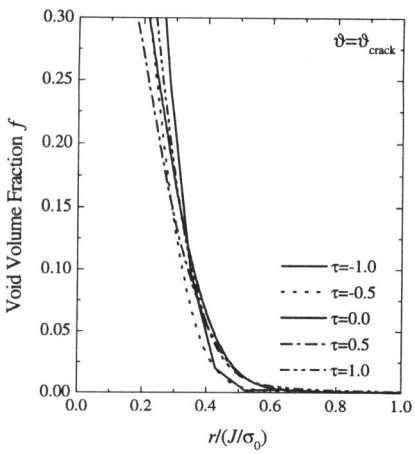

Figure 4: Radial distributions of the void volume fraction around the tip under different applied transverse T-stresses at $\vartheta = \vartheta_{crack}$. The mesh contains 24 quadratic element sectors around the tip.

The prediction about the crack growth angle is not contradictory to known computational results. With further increasing the applied loads the crack growth turns to the symmetrical plane and the kinking occurs just at the very begin of the crack growth ($\Delta a \leq 2\delta_0$). Should the finite elements be as large as the initial blunting radius [14] this small kinking cracking can be simply suppressed.

Furthermore, the transverse stress changes not only the crack growth angle but also evolution of the damage zone around the crack tip. In Fig. 2 we find that for the same applied J values the total damage amount of the material which is proportional to the areas below the curves increases with T. It means that a negative T stress will make less material in the crack tip field damaged under the same applied crack drive force. It tentatively explain why the crack with higher constraints, i.e. $T > 0$, initiates at a lower applied J value and vice versa.

The length of the damage zone at $\vartheta = \vartheta_{crack}$ is hardly effected by the applied T stresses. Fig. 4 shows radial distributions of the void volume fraction along the crack growth directions. As known in strain localization analyses, the width of the high damage zone corresponds to the element size which implies the known mesh dependence in local mechanics. The results in Fig. 4 implies that the prediction of the crack growth amount is sensitive to the FE mesh.

CONCLUSIONS

The crack tip fields have been studied using different finite element meshes. According to the present computations the numerical results are essentially determined by the initial blunting radius of the crack tip. All numerical predictions are scalable with the blunting radius.

Using most different meshes we have confirmed that the crack does not initiate along the symmetrical plane and the crack growth angle at initiation can be approximated by a third-order polynomial. The crack angle increases with the T stress. Furthermore, T promotes material damage around the crack tip under the same applied J value. Under small-scale yielding conditions the present results confirm the two-parameter characterizations based on continuum mechanics.

REFERENCES

[1] Parks, D. M. (1992). In *Topics of Fracture and Fatigue*, edited by A. S. Argon, Springer Verlag New York, pp. 59-98.

[2] O'Dowd, N. P. and Shih, C. F. (1991). *J. Mech. Phys. Solids*, **39**, pp. 989-1015.

[3] Faleskog, J. (1995). *J. Mech. Phys. Solids*, **43**, pp. 447-493.

[4] Yuan, H. and Brocks, W. (1998). *J. Mech. Phys. Solids*, **46**, pp 219-241.

[5] Brocks, W. & Schmitt, W. (1994). Constraint Effects in Fracture Theory and Applications: Second Volume. ASTM STP 1244, (M. T. Kirk and A. Bakker, eds.), American Society for Testing and Materials, Philadelphia, pp. 209-231.

[6] Al-Ani, A. M. and Hancock, J. W. (1991). *J. Mech. Phys. Solids*, **39**, pp. 23-43.

[7] Betegón, C. and Hancock, J. W. (1991). Transaction of ASME, *J. Appl. Mech.*, **58**, pp. 104-110.

[8] Gurson, A. L. (1977). *J. Eng. Mat. Techn.*, **99**, pp. 2-15.

[9] Tvergaard, V. (1990). *Advances of Applied Mechanics*, **27**, pp. 83-151.

[10] Needleman, A. and Tvergaard, V. (1987). *J. Mech. Phys. Solids*, **35**, pp. 151-183.

[11] Fleck, N. A. and Hutchinson, J. W. (1997). *Advances of Applied Mechanics*, **33**, pp. 295-361.

[12] Sun, D.-Z., and Hönig, A. (1994). in *Proc. 3rd Int. Conf. on Localized Damage*, ed. M. H. Aliabadi etc. Comp. Mechanics Publication, Southampton, pp. 287-296.

[13] Barenblatt, G. I. (1996). Scaling, self-similarity, and intermediate asymptotics. Cambridge University Press.

[14] Xia, L. and Shih, C. F. (1995). *J. Mech. Phys. Solids*, **43**, pp. 233-259.